



Original Article

DOI: 10.36959/525/450

Paclitaxel-Copper Composite: A Metallodrug Model System Enroute Ultrasonic Force

Amol A Shedge¹, Shubham V Pansare^{1,2}, Dnyaneshwar K Kulal¹, Shyam R Khairkar¹, Shraddha Y Chhatre³, Debiprasad Panda², Maryappa C. Sonawale⁴, S Chakrabarti^{2*}, Amol V Pansare^{2,4*} and Vishwanath R Patil^{1*}

¹Department of Chemistry, University of Mumbai, Santacruz (E), Mumbai, India

²Department of Electrical Engineering, Indian Institute of Technology Bombay (IITB), Mumbai, India

³National Chemical Laboratory (NCL) Dr. Homi Bhabha Road, Pune, India

⁴Veer Wajekar Arts Science and Commerce College, Navi Mumbai 400702, India

⁵Composites group, Mechanical Systems Engineering, Swiss Federal Laboratories for Materials Science and Technology-Empa, Dübendorf, Switzerland



Abstract

Paclitaxel (PTX), an anti-microtubule agent, widely used as an efficacious anti-neoplastic drug in the treatment of numerous cancer diseases. The major disadvantage of PTX drug is practical insolubility in aqueous media and poor bioavailability, which directly impacts drug absorption in human beings. In this research, we successively tried to increase the bioavailability of PTX, by synthesizing PTX-Copper nanocomposite (Cu NCP) using water bath type ultrasonication method. PTX-Cu NCP exhibited significantly higher solubility in different aqueous media as compared to plain PTX. The drug release profile of PTX-Cu NCP was also comparatively positive with respect to plain PTX. PTX-Cu NCP was well characterized by SEM, XRD, UV-Vis spectroscopy and zeta potential. Physico-chemical properties and biological behavior of BSA- PTX-Cu NCP were evaluated by emission spectroscopy, where the binding constant was found to be 4.76×10^2 . Negative values of enthalpy [$\Delta H^\circ = -49.52 \text{ kJmol}^{-1}$] and entropy [$\Delta S^\circ = -113.14 \text{ Jmol}^{-1}\text{K}^{-1}$] indicate hydrophilic interaction between BSA and PTX-Cu NCP. Circular Dichroism binding studies of PTX-Cu NCP suggests no major change in secondary structure of BSA protein. PTX-Cu NCP displays favorable antioxidant activity with respect to ascorbic acid and comparatively prominent anticancer activity on MCF-7 and COLO-205 cell lines against standard anticancer drug ADR (Adriamycin) (Graphical abstract).

Keywords

Nanocomposites synthesis, Metallodrugs, Cancer activity, Copper, Fluorescence

Introduction

In the recent decade, breast cancer is a lethal carcinoma which is prevalent worldwide in women. Colon cancer is the second extremely dangerous cancer in males as well as females claiming the life of patients in developed as well as developing countries. In 2019, due to cancer 9.6 million deaths have occurred and 18.1 million new cases of cancer have been detected [1,2]. Generally, standard cytotoxic chemotherapy is the first line of treatment given to cancer patients. A number of plant-derived synthetic drugs alone or in combination have been used in cancer treatment such as Doxorubicin, Cis-Platin, Paclitaxel, Capecitabine and Curcumin [3-7]. Paclitaxel (PTX), a natural diterpenoid, isolated from the bark of Pacific Yew tree is used for treating number of cancer such as breast, ovarian, pancreatic and cervical cancer [8-10]. The main drawback of hydrophobic PTX is low solubility and

***Corresponding author:** Vishwanath R Patil, Department of Chemistry, University of Mumbai, Santacruz (E), Mumbai 400098, India;

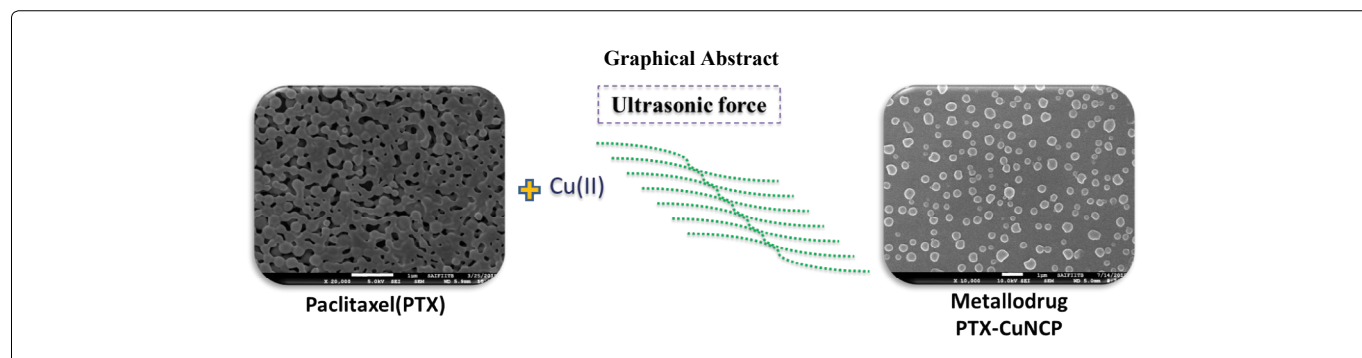
Amol V Pansare, Composites group, Mechanical Systems Engineering, Swiss Federal Laboratories for Materials Science and Technology-Empa, 8600 Dübendorf, Switzerland;

S Chakrabarti, Department of Electrical Engineering, Indian Institute of Technology Bombay (IITB), Mumbai, India

Accepted: September 18, 2021

Published online: September 20, 2021

Citation: Shedge AA, Pansarea SV, Kulal DK, et al. (2021) Paclitaxel-Copper Composite: A Metallodrug Model System Enroute Ultrasonic Force. *Current Trends Anal Bioanal Chem* 5(1):158-166



bioavailability, higher cytotoxicity and tendency to crystallize in aqueous conditions. To increase the bioavailability of PTX we need to decrease the particle size and increase hydrophilicity [11]. Numerous strategies have been reported such as PTX functionalized gold nanoparticles, herceptin-bearing PTX loaded nanoparticles [12,13], lipid nanovesicle aerosol which improved the efficacy of PTX in lung cancer [14], PTX loaded lipid nanoparticles which were formulated using a modified solvent injection technique [15], and PTX incorporated polymer prodrug strategies [16,17]. Nanoparticles of PTX using PEG/PHO were utilized for antitumor drug delivery [18], production of aqueous nano colloids of PTX [19], PTX/Chitosan nanosuspensions for enhanced intravesical cancer therapy and prolonged delivery of PTX have also been reported [20]. Researchers also synthesized some metal complexes of PTX viz; PTX-nanodiamond nanocomplex [21], Paclitaxel loaded-BSA nanoparticles for brain tumor targeting [22]. To overcome the bioavailability and solubility issue, novel Paclitaxel pharmaceutical formulations such as Cremophor-EL, Abraxane, Taxopreïn, Paclicalpoliglumex, ANG1005, Paccal have been developed in the recent decade [23,24]. For the synthesis of the reported organ metallic nanoparticles and nano composites of PTX, various physical methods of stirring, centrifugation, etc were reported, wherein the use of metal oxide for complex formation via coordinate bonding or covalent bonding between metal and drug molecule. Such composites exhibit anti-cancer activity, but their bioavailability is low and hence there is a need to synthesize a new moiety which is only electrostatic ally bonded via Vander Wall forces. Copper, a biologically essential element, in the form of nanoparticles has diversified areas such as biocatalysis, antibacterial activity, anti-biofouling activity, antioxidant and anticancer activities [25-28]. For human beings the recommended orally dietary intake of copper from food is 0.9 mg/day and the tolerable upper intake level of copper is 10.0 mg/day [29]. The median lethal dose (LD50) of copper nanoparticles is 413 mg/kg of human body weight and considered as moderately toxic materials hence we used Cu metal for NCP synthesis [30]. The insolubility of PTX poses a major hurdle in drug development; hence use of PTX alone in aqueous based anticancer pharmaceutical formulations is not feasible [31]. The solubility, bioavailability and dissolution of a drug are correlated to its particle size, which further plays an important role in drug absorption at the specific targeted site [32-34]. Lower the particle size, higher is the drug absorption because more number of atoms are exploited at the surface and higher the particle size lower is the rate of drug absorption

[35]. Ultrasonic sonochemistry is a high energy interaction of energy and matter through acoustic cavitation leading to agitation of particles or collapse of bubbles in liquid wherein sound waves transform into mechanical energy to complete a reaction [36].

Hence, we decided to use a simple, cost efficient, less time consuming ultrasonication technique for the synthesis of PTX-Cu NCP. We developed a novel strategy for increasing the bioavailability and solubility of PTX by using simple water bath ultrasonication at ambient temperature. In this work we synthesized the PTX-Cu NCP by mixing Paclitaxel and copper oxide in a 1:1 mole ratio.

Experimental Section

Materials and methods

The Paclitaxel (PTX) drug was bought from Sigma Aldrich and Ethanol from Merck. Copper oxide was procured from Sigma Aldrich. Anticancer activity on MCF-7 (Breast) and COLO-205 (Colon) cancer cell lines by SRB Assay method were performed at ACTREC (Kharghar, Navi-Mumbai, India). Free radical scavenger DPPH Assay method was used for evaluating the antioxidant activity.

Synthesis of PTX-Cu NCP

PTX and copper oxide (stoichiometric 1:1 mole ratio) were transferred in 50 ml ethanol, sonicated in water-bath type ultrasonicator (Soltec Sonica ultrasonic cleaner) at ambient temperature for 30 mins. Then the reaction mixture was centrifuge at 45000 rpm for 10 mins and unreacted metal part was separate from the main nanocomposite. The supernatant solution was first air dried and further dried in hot air vacuum oven at 105 °C, thus obtaining Paclitaxel-copper nanocomposite (PTX-Cu NCP).

Characterization of PTX-Cu NCP

The PTX-Cu NCP were characterized by FEG-SEM, JEOL model JSM-7600F with 30 kV accelerating voltage in vacuum [37,38]. UV-Vis spectroscopy (LAB UV3000plus) was used to examine the reaction during sonication to monitor the reduction of copper ions to copper nanoparticles with PTX. The range of 200-800 nm was selected by utilizing ethanol as blank. The X-ray diffraction(XRD) scans for PTX-Cu NCP were carried out employing Shimadzu maxima 7000 X-ray diffract meter bearing 5° to 80° probing range. Zeta potential was studied by dynamic light scattering [Malvern, Instrument Ltd].

Solubility study of PTX-Cu NCP

The solubility study was performed freshly prepared 0.1N HCl (pH 1.2), 50 mM sodium acetate buffer (pH 4.5), 50 mM potassium phosphate buffer (pH 6.8) and 50 mM phosphate buffer saline solution (pH 7.2), methanol, ethanol, dimethyl sulfoxide, water and its each of solvent mixtures (1:1 ratio) of water methanol, water ethanol, water:dimethyl sulfoxide [39]. Standard solution of PTX was prepared in DMSO for comparison with various medias of PTX-Cu NCP. Weighed and transferred 20 mg each of PTX and PTX-Cu NCP into 200 ml volumetric flask, then added respective media (Table S1) and respective solutions were stirred on mechanical shaker at 100 revolutions per minute in an ambient temperature for 24 hrs, then each of the flask were diluted to volume with respective media and absorbance of these solutions was read using LAB UV3000^{plus} at 227 nm by utilizing respective media as blank.

Drug releasing study

The drug release study was carried out *in-vitro* using water bath type dissolution apparatus operated at 37 °C. Thin pellets of PTX and PTX-Cu NCP were prepared using pellet press assembly and then added in dissolution jars containing phosphate buffer saline solution (50 mM PBS pH 7.2). The drug releasing profile was studied for 24 hours at various time intervals and the absorbance of this solution was recorded at 227 nm, PBS solution was used as blank for UV measurement.

BSA Binding studies

UV-Vis. absorption measurements were carried out using a LAB UV3000plus equipped with quartz cell cuvette having path-length of 1 cm as a sample holder. 2.5% DMSO-5 mM pH-7.2 Tris-HCl buffer was used for preparing stock solutions of PTX, copper oxide and PTX-Cu NCP to required concentrations for BSA absorption studies. Tris-HCl buffer used as blank for absorption measurements.

Emission measurements of unstable complex BSA-PTX-Cu NCP were probed on RF-5301PC SHIMADZU spectrofluorophotometer. The emission bands were recorded from 250 nm to 700 nm at an excitation wavelength of 278 nm. BSA solution (1.5×10^{-5} M) was prepared in 5 mM Tris-HCl buffer. The required concentration stock solutions of PTX-Cu NCP in 2.5% DMSO-5 mM pH-7.2 Tris-HCl buffer were prepared and further diluted to required concentrations for all emission studies with BSA. Tris-HCl buffer was used as control for fluorescence measurements. Using the stock solution (1.12×10^{-4} M) of PTX-Cu NCP different concentrations of PTX-Cu NCP solutions (2.81×10^{-6} M to 1.41×10^{-5} M) was produced.

The CD (JASCO, J-815 CD spectrometer) analyses were performed in the UV range of 200-260 nm.

Scavenging activity

DPPH antioxidant activity of PTX-Cu NCP was determined using Brand-Willas method [40].

In vitro cytotoxicity studies of the PTX-Cu NCP

In-vitro anticancer activity was studied for PTX-Cu NCP

by SRB assay method using MCF-7 and COLO-205 [41]. MCF-7 and COLO-205 were propagated in RPMI-1640 medium containing 10% fetal bovine serum and 2 mM L-glutamine at 37 °C humidified atmosphere of 5% CO₂ in the air. Sulphorhodamine B (SRB) based *in vitro* cytotoxicity assay was performed to compare anticancer effects of PTX, PTX-Cu NCP and ADR against MCF-7 and COLO-205 cell line. Different concentrations of PTX, PTX-Cu NCP solutions and Adriamycin (positive control drug) viz. 10 µg/ml, 20 µg/ml, 40 µg/ml and 80 µg/ml were produced by serial dilution of stock solution. The detailed procedure of cell viability and SRB staining (See Supporting Information section) was followed as per previously reported method by Pansare, et al. [42].

Results and Discussion

Synthesis of PTX-Cu NCP

Ultrasonication [43] plays an important role in synthesis of PTX-Cu NCP. We first time reported the PTX-Cu NCP by sonication method. The nano composite were synthesized using PTX and copper oxide suspended in ethanol using simple water bath type ultrasonicator. The ultrasonically synthesized PTX-Cu NCP were further evaluated for UV-Vis, SEM, XRD and zeta potential studies.

Characterization studies

UV-Vis. absorption scans were evaluated in the range of 200-800 nm [44]. The comparative UV-Vis spectra of PTX, ultrasonically synthesized PTX-Cu NCP of required concentrations in ethanol were shown in Figure S1. A slight shift in the wavelength maxima of the PTX-Cu NCP as compared to PTX shows complex formation of PTX with copper. This wave length shift also indicates that there is a reduction of copper, resulting in the formation of a nano composite. Functional groups such as amines, hydroxyl and alkyl groups present in PTX molecule can act as reducing agents to reduce copper ion [45-47]. In the previously reported data of PTX [48-50], the particles of the drug appear to bound together/agglomerated (Figure 1a - Figure 1b). The SEM morphology of PTX-Cu NCP (Figure 1c - Figure 1d) first time proves that due to ultrasonication, the circular nanoparticles separate from each other and are well-dispersed. In the previously reported articles, various types of commercially available PTX nanoparticles are clubbed together wherein the particle size is higher as compared to ultrasonically synthesized PTX-Cu NCP [51-53]. The reduced agglomeration of PTX can result in increased solubility, correspondingly boosting its bioavailability observed towards ultrasonically synthesized PTX-Cu NCP. The distinct diffraction peaks [54] of PTX (-Cu NCP are shown in Figure 2. The apparent zeta potential was -30 mV for PTX-Cu NCP as shown in Figure S2.

Solubility study of PTX-Cu NCP

The solubility study in various media viz. water, organic solvents and buffers in terms of concentrations calculated in mg/ml were shown in the Figure 3 and Table S1. Solubility data concluded that, PTX-Cu NCP was more soluble as compared to plain PTX in various media solutions.

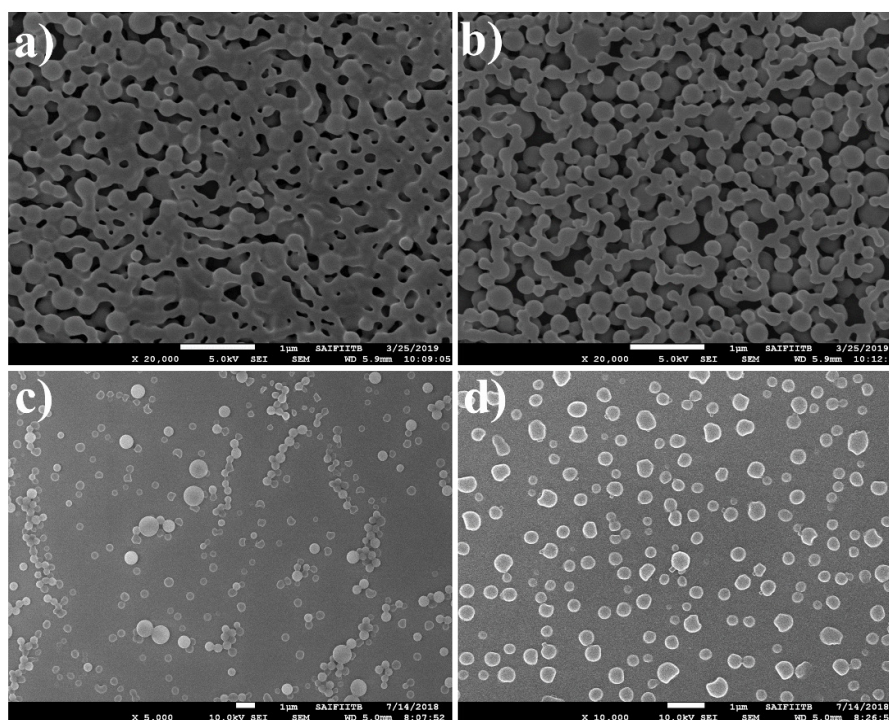


Figure 1: (a,b) SEM morphology of PTX; (c,d) PTX-Cu NCP.

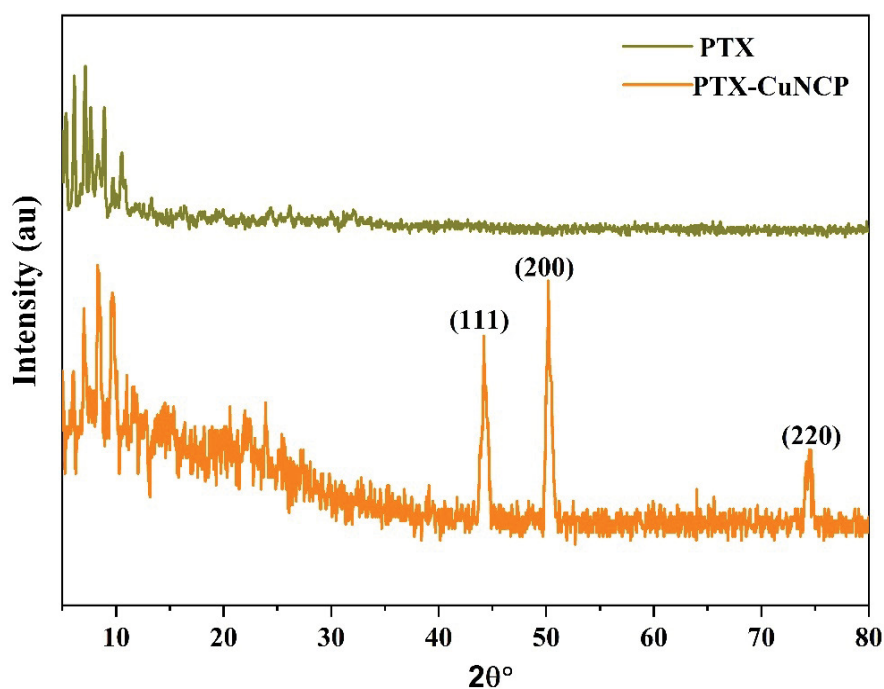


Figure 2: X-ray diffraction pattern of PTX-Cu NCP.

Drug release profile study

The drug release profile study of PTX-Cu NCP and PTX studied at various time intervals till 24 hours is shown in Figure 4 and Table S2. The % drug release of PTX-Cu NCP was faster as compared to plain PTX.

BSA Interaction studies with PTX-Cu NCP

UV-Vis absorption studies: For detecting the complex formation between metal and BSA, UV-Vis. absorption spectroscopy is the important method wherein structural or conformational changes in BSA environment can be monitored [55]. Figure S3 demonstrates the absorption of

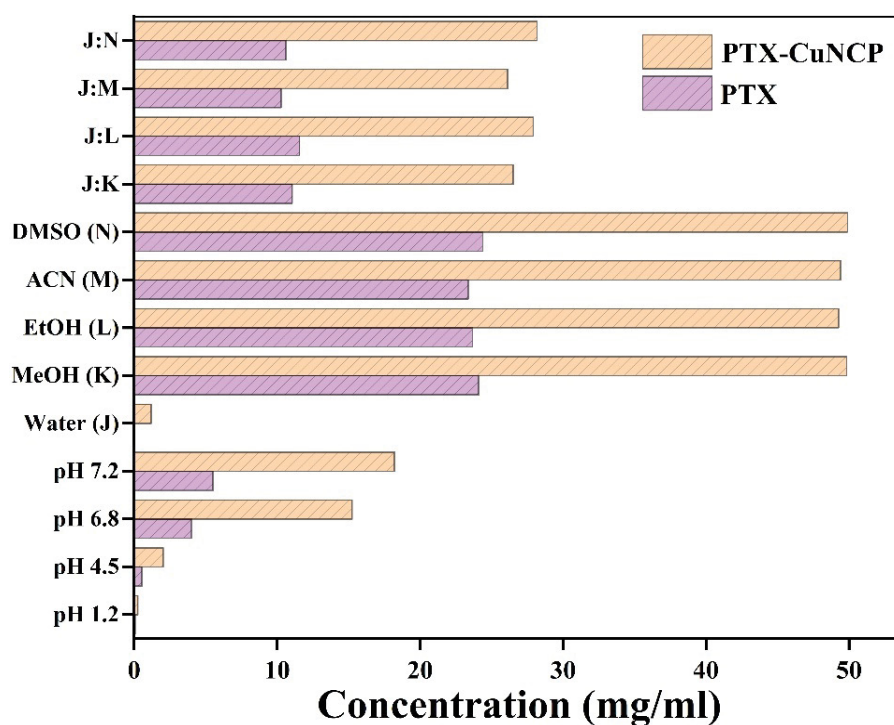


Figure 3: Solubility study of PTX and PTX-Cu NCP in various media.

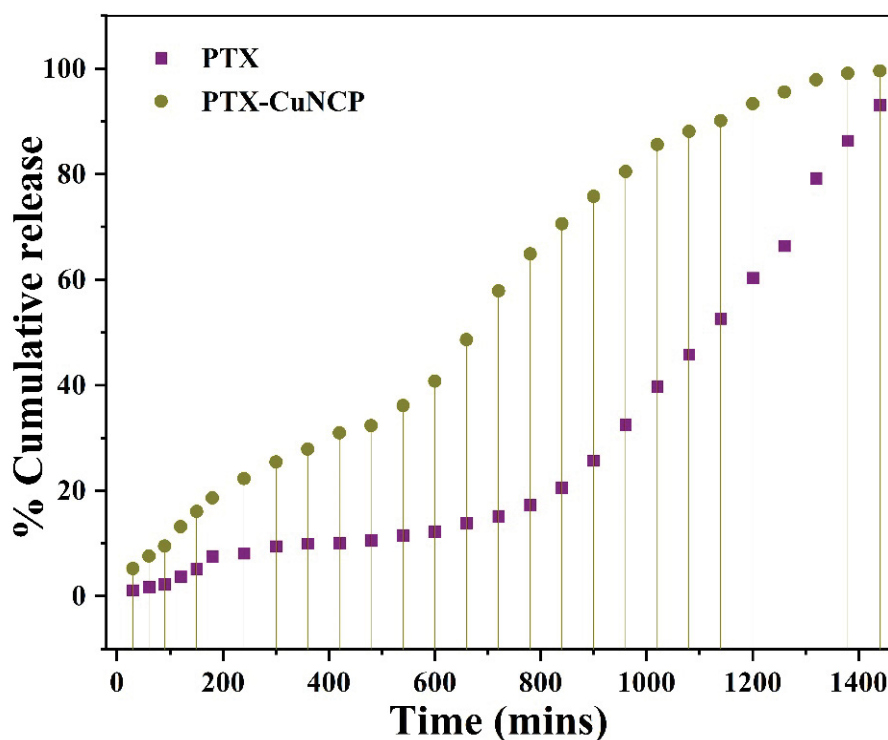
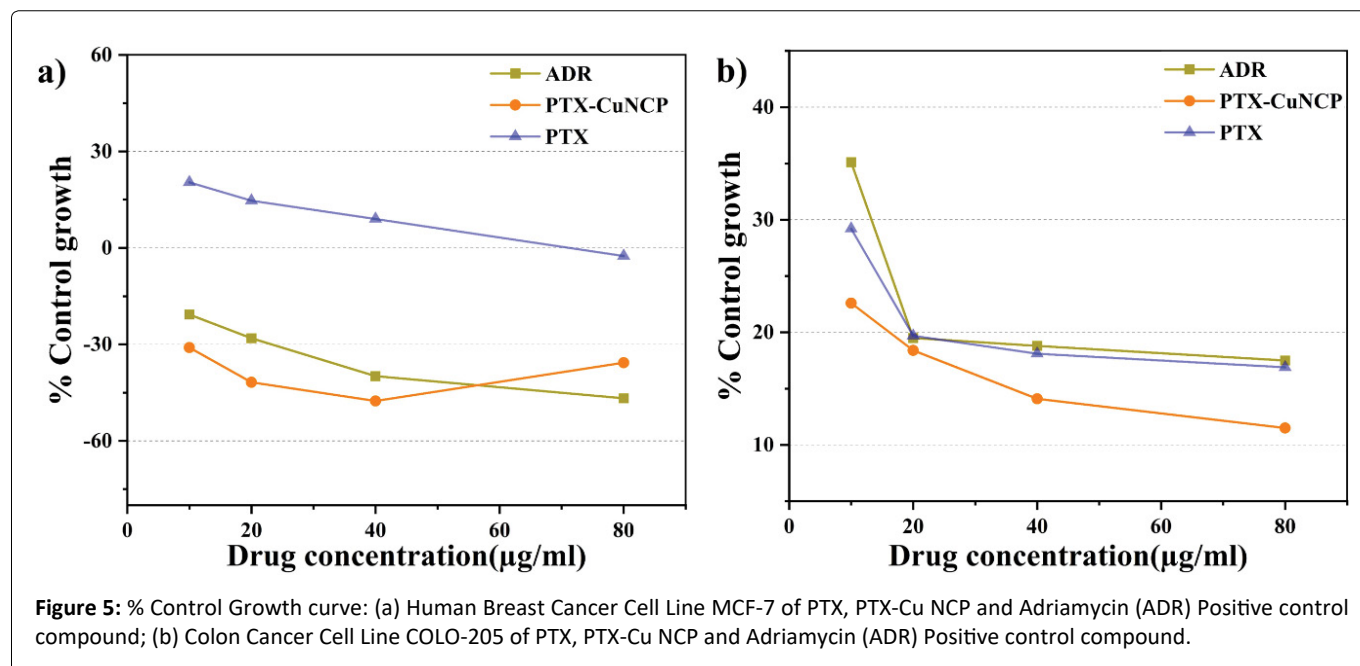


Figure 4: Comparative drug release profile of PTX and PTX-Cu NCP.

BSA in existence of PTX-Cu NCP, the assimilation magnitude of BSA escalates with the increasing amount of PTX-Cu NCP indicating the complex formation wherein the interaction process is static quenching.

Fluorescence quenching studies: Interactivity amongst quencher (small molecule) with BSA occurs by dynamic and static quenching. The emission intensity investigated for distinguishing between these two types of quenching behaviors. The diffusion rate of the quencher surges as the



temperature elevates which results in a greater possibility of the dynamic type quenching [56-60]. Emission quenching behavior between BSA and PTX-Cu NCP was inscribed for free BSA and compounded with distinct concentration of PTX-Cu NCP at temperatures of 293K, 298K, and 310K. As indicated in the Figure S4- Figure S6 at an excitation wavelength of 278 nm, BSA exhibits an exigent emission band at 345 nm. Emission spectrum of BSA diminishes with increasing concentration of PTX-Cu NCP (2.81×10^{-6} M to 1.41×10^{-5} M) which indicates static interaction. The quenching data probed by Stern-Volmer equation ($F_0/F = 1 + K_{sv} [Q] = 1 + k_q T_0 [Q]$), F_0 and F express fixed condition emission in nonexistence and existence of PTX-Cu NCP accordingly. K_{sv} is the Stern-Volmer constant, and $[Q]$ is the concentration of PTX-Cu NCP, k_q is the quenching rate factor and T_0 is the mean lifespan of protein except any quencher. The Stern-Volmer plot of F_0/F vs $[Q]$ displayed in Figure S7 and slope of this plot gains the Stern-Volmer constant (Table S3). The association amidst the BSA and PTX-Cu NCP emerges through a static quenching process, which was confirmed because the quenching constant k_q was in the succession of 10^{11} . Binding constant (K) and number of binding sites (n) amongst the quencher and BSA is calculated by: $\log (F_0 - F)/F = \log K + n \log [Q]$. The value of n and K were gained from the slope and Y axis intercept appropriately by straight befitting the plot of $\log [(F_0 - F)/F]$ vs. $\log [Q]$ [61] (Figure S8). Table S3 summarizes this value as a function of temperature and it exposes that K and n decreased with the surge in temperature, forming an unstable complex of PTX-Cu NCP with BSA. Drugs usually bind to the macromolecule through different types of intermolecular forces such as hydrogen bonding, Vander Waals forces and electrostatic interactions. The change in enthalpy (ΔH°) and entropy (ΔS°) was obtained from Vant Hoff's equation [$\ln K = (-\Delta H^\circ/RT) + (\Delta S^\circ/R)$], where T temperature, R Gas constant, K binding constant. Gibbs free energy is figured from $\Delta G^\circ = \Delta H^\circ - T\Delta S^\circ = -RT \ln K$. From the plot of $\ln K$ vs. $1/T$, ΔH° and ΔS° calculated from the slope and intercept respectively (Figure S9). The

values of ΔG° , ΔH° and ΔS° are described in Table S4, the negative values of ΔS° ($-113.14 \text{ Jmol}^{-1}\text{K}^{-1}$) and ΔH° ($-49.52 \text{ KJmol}^{-1}$) clearly indicates that, in the binding process of PTX-Cu NCP-BSA hydrophilic interaction depicts a crucial aspect. The value of ΔG° illustrated that interaction between PTX-Cu NCP and BSA occurred spontaneously.

CD Spectroscopy: Circular Dichroism (CD) spectroscopic technique is useful for monitoring the interaction between protein and drugs. The conformational changes are induced into the protein due to the interaction between BSA and PTX-Cu NCP for which the intramolecular forces are responsible for the alteration of secondary and tertiary structures of BSA [62]. The far UV region (195-245 nm) is employed to explore the concomitant anatomy of protein, where the peptide link is accountable for UV absorption. The spectral magnitude of BSA diminishes with the inclusion of PTX-Cu NCP as presented in Figure S10. The CD findings are asserted in terms of molar residual ellipticity (MRE) using equations reported by Pansare, et al. [55]. The results of α -helical anatomy of free and bound BSA at 208 and 222 nm were evaluated using the equations reported by Stan, et al. [62]. In Table S5, the % of α -helix values is revealed. The peak shape and peak maximum remained almost same but the percent α -helicity diminished from 63.95% to 57.40% at 208 nm and 53.75% to 48.38% at 222 nm signifying the alteration in secondary network of BSA during interaction with PTX-Cu NCP. This discloses that BSA holds α -helix configuration after binding to PTX-Cu NCP.

Scavenging activity

DPPH free radical scavenging activity is a basic method for the estimation of antioxidant activity [63]. Ethanolic solution of DPPH: 2,2-diphenyl-1-picrylhydrazyl, (2.16 mg/50 ml), standard antioxidant Ascorbic acid (100 µg/ml) and PTX-Cu NCP (100 µg/ml) were produced. Solutions of 5, 10, 15, 20, 25 µg/ml were prepared by serial dilution of each of stock solutions of ascorbic acid and PTX-Cu NCP. 5 ml each of DPPH solution and ascorbic acid solution were incubated

at room temperature in a dark atmosphere for 30 mins and absorbance was noted immediately thereafter at 517 nm. Similarly ethanolic PTX-Cu NCP solution was treated with DPPH and absorbance was recorded at 517 nm. % Scavenging activity was calculated by equation as reported by Pyrzynska, et al. [63] increasing antioxidant activity with increase in concentration of PTX-Cu NCP with respect to ascorbic acid are shown in Figure S11 and Table S6. The possession of antioxidant activity implies that PTX-Cu NCP can exhibit profound anti proliferation activity as discussed in further section.

In-vitro anticancer activity

PTX-Cu NCP shows prominent anticancer activity on MCF-7 and COLO-205 in comparable with PTX and standard anticancer drug ADR. Anticancer activity of the PTX-Cu NCP against respective cell lines were analyzed in terms of GI50 (Concentration of drug causing 50% inhibition of cell growth), TGI (Concentration of drug causing total inhibition of cell growth) and LC50 (Concentration of drug causing 50% cell kill) values [42]. All the SRB (Sulphorhodamine B) assays were evaluated in triplicate (no. of samples, n = 3) at various concentrations. Table S7, Table S8, Table S9 and Table S10 summarizes the anticancer data acquired by assay. PTX-Cu NCP were established to be the profoundly functional anticancer substance inducing > 50% inhibition of MCF-7 and COLO-205 cell escalation at amounts < 10 µg/ml. The resultant Figure 5a, Table S7 and Table S9 displays PTX-Cu NCP possess comparatively high substantial anti-carcinoma activity versus MCF-7 in comparison with PTX. Figure 5b, Table S8 and Table S10 demonstrated that, PTX-Cu NCP have high significant anticancer activity against COLO-205 in comparison with PTX. The GI50 value observed for PTX-Cu NCP was comparable with standard anti-cancer drug ADR (Positive control compound).

Conclusion

Erstwhile researchers demonstrated to enhance the hydrophilic properties of PTX conjugates, wherein PTX drug cannot be efficiently absorbed in homogeneous manner on the site of action. Here we successively developed the strategy to enhance hydrophilic character of PTX-Cu NCP by simple ultrasonic energy, wherein the decisive SEM morphology of PTX-Cu NCP was evenly distributed as compared to PTX. We herein strongly conclude that spontaneous interaction between BSA-metallodrug PTX-Cu NCP suggested hydrophilic binding as compared to hydrophobic PTX. PTX-Cu NCP shows good antioxidant activity due to which they exhibit prominent anticancer activity on MCF-7 and COLO-205 in correlation to standard anticancer drug ADR. Prominently high solubility in different aqueous media and comparatively greater drug release profile of PTX-Cu NCP with respect to plain PTX, signifies that PTX-Cu NCP can be profoundly used in the targeted drug delivery systems like, nano-biomedical fields and in pharmaceutical compositions/formulations replacing existing PTX.

Acknowledgements

The author (Amol A Shedge) acknowledges Department of

Chemistry, University of Mumbai for its technical support for carrying out this research and authors (Shubham V Pansare, Amol V Pansare) acknowledges National Centre of Excellence in Technologies for Internal Security (NCETIS), IRCC IITB, Mumbai, India for providing resources and infrastructure facility in carrying out this research.

Highlights

- Synthesis of copper metal containing paclitaxel: Metallodrug PTX-Cu NCP.
- Greater solubility and drug release properties of metallodrug PTX-Cu NCP as compared to PTX.
- Interaction of protein BSA with PTX-Cu NCP in the favour of bioavailability.
- Anticancer activity of hydrophobic paclitaxel elevated in the hydrophilic metallodrug PTX-Cu NCP.

References

1. Bray F, Ferlay J, Soerjomataram I, et al. (2018) Global cancer statistics 2018: GLOBOCAN estimates of incidence and mortality worldwide for 36 cancers in 185 countries. *CA Cancer J Clin* 68: 394-424.
2. Siegel RL, Miller KD, Jemal A (2019) Cancer Statistics, 2019. *CA Cancer J Clin* 69: 7-34.
3. Xu P, Zuo H, Chen B, et al. (2017) Doxorubicin-loaded platelets as a smart drug delivery system: An improved therapy for lymphoma. *Sci Rep* 7: 42632.
4. Dasari S, Tchounwou PB (2014) Cisplatin in cancer therapy: Molecular mechanisms of action. *Eur J Pharmacol* 740: 368-374.
5. Zhao X, Fan J, Wu P, et al. (2019) Chronic chemotherapy with paclitaxel nanoparticles induced apoptosis in lung cancer in vitro and in vivo. *Int J Nanomedicine* 14: 1299-1309.
6. Hirsch BR, Zafar SY (2011) Capecitabine in the management of colorectal cancer. *Cancer Manag Res* 3: 79-89.
7. Li Y, Zhang T (2014) Targeting cancer stem cells by curcumin and clinical applications. *Cancer Lett* 346: 197-205.
8. Singla K, Garg A, Aggrawal D (2002) Paclitaxel and its formulations. *Int J Pharm* 235: 179-192.
9. Baloglu E, Kingston DG (1999) The taxane diterpenoids. *J Nat Prod* 62: 1448-1472.
10. Rowinsky EK, Donehower RC (1995) Paclitaxel (Taxol). *N Engl J Med* 332: 1004-1014.
11. Sharma S, Verma A, Teja BV, et al. (2014) Development of stabilized paclitaxel nanocrystals: In-vitro and in-vivo efficacy studies. *Eur J Pharm. Sci* 69: 51-60.
12. Gibson JD, Khanal BP, Zubarev ER (2007) Paclitaxel functionalized gold nanoparticles. *J Am Chem Soc* 129: 11653-11661.
13. Yu K, Zhou Y, Li Y, et al. (2016) Comparison of three different conjugation strategies in the construction of herceptin-bearing paclitaxel-loaded nanoparticles. *Biomaterials Science* 4: 1219-1232.
14. Joshi N, Kaviratna A, Banerjee R (2013) Multi trigger responsive, surface active lipid nanovesicle aerosols for improved efficacy of paclitaxel in lung cancer. *Integr Biol (Camb)* 5: 239-248.

15. Pandita D, Ahuja A, Velpandian T, et al. (2009) Characterization and in vitro assessment of paclitaxel loaded lipid nanoparticles formulated using modified solvent injection technique. *Pharmazie* 64: 301-310.
16. Louage B, Nuhn L, Risseuw MDP, et al. (2016) Well-defined polymer-paclitaxel prodrugs by a grafting-from-drug approach. *Angew Chem Int Engl* 55: 11791.
17. Lewis RW, Evans RA, Malic N, et al. (2018) Ultra-fast aqueous polymerisation of acrylamides by high power visible light direct photo activation RAFT polymerisation, *Polymer Chemistry* 9: 60-68.
18. Kim HY, Ryu JH, Chu CW, et al. (2014) Paclitaxel-incorporated nanoparticles using block copolymers composed of poly (ethylene glycol)/poly (3-hydroxyoctanoate). *Nanoscale Res Lett* 9: 525.
19. Pattekari P, Zheng Z, Zhang X, et al. (2011) Top-down and bottom-up approaches in production of aqueous nanocolloids of low solubility drug Paclitaxel. *Physical Chemistry Chemical Physics* 13: 9014-9019.
20. Liu Y, Wang R, Hou J, et al. (2018) Paclitaxel/chitosan nanosuspensions provide enhanced intravesical bladder cancer therapy with sustained and prolonged delivery of Paclitaxel. *ACS Appl Bio Mater*.
21. Lim DG, Jeong JH, Ko HW, et al. (2016) Paclitaxel-nanodiamond nanocomplexes enhance aqueous dispersibility and drug retention in cells. *ACS Appl Mater Interfaces* 8: 23558-23567.
22. Bansal A, Kapoor DN, Kapil R, et al. (2011) Design and development of paclitaxel-loaded bovine serum albumin nanoparticles for brain targeting. *Acta Pharm* 61: 141-156.
23. Nehate, Jain S, Saneja A, et al. (2014) Paclitaxel formulations: challenges and novel delivery options. *Curr Drug Deliv* 11: 666-686.
24. Marupudi NI, Han JE, Khan LW, et al. (2007) Paclitaxel: A review of adverse toxicities and novel delivery strategies. *Expert Opin Drug Saf* 6: 609-621.
25. Manning T, Slaton C, Myers N, et al. (2018) A Copper¹⁰-Paclitaxel crystal; a medically active drug delivery platform. *Bioorganic Med Chem Lett* 20: 3409-3417.
26. Kimber RL, Lewis EA, Parmeggiani F, et al. (2018) Biosynthesis and characterization of copper nanoparticles using *Shewanella oneidensis*: Application for Click Chemistry. *Small* 14.
27. Mahmoodi S, Elmi A, Hallaj-Nezhadi S (2018) Copper nanoparticles as antibacterial agents. *J Mol Pharm Org Process Res* 6: 140.
28. Din MI, Arshad F, Hussain Z, et al. (2017) Green adeptness in the synthesis and stabilization of copper nanoparticles: Catalytic, antibacterial, cytotoxicity, and antioxidant activities. *Nanoscale Res Lett* 12: 638.
29. Taylor, Tsuji JS, Garry MR, et al. (2020) Critical review of exposure and effects: Implications for setting regulatory health criteria for ingested copper. *Environ Manage* 65: 131-159.
30. Hejazy M, Koochi MK, Bassiri APM, et al. (2018) Toxicity of manufactured copper nanoparticles-A review. *Nanomedicine Research Journal* 3: 1-9.
31. Ma P, Mumper RJ (2013) Paclitaxel nano-delivery systems: A comprehensive review. *J Nano Med Nano Technol* 4: 1000164.
32. Rijt SHV, Bein T, Meiners S (2014) Medical nanoparticles for next generation drug delivery to the lungs. *Eur Respir J* 44: 765-774.
33. Khadka P, Roa J, Kim H, et al. (2014) Pharmaceutical particle technologies: An approach to improve drug solubility, dissolution and bioavailability. *Asian Journal of Pharmaceutical Sciences* 9: 304-316.
34. Pal Y, Deb PK, Bandopadhyay S, et al. (2018) Chapter 3 - role of physicochemical parameters on drug absorption and their implications in pharmaceutical product development. *Dosage Form Design Considerations* 85: 116.
35. Sun J, Wang F, Sui Y, et al. (2012) Effect of particle size on solubility, dissolution rate, and oral bioavailability: Evaluation using coenzyme Q10 as naked nanocrystals. *Int J Nanomedicine* 7: 5733-5744.
36. Suslick KS (1990) Sonochemistry. *Science* 247: 1439-1445.
37. Pansare V, Khairkar SR, Shedge AA, et al. (2018) In situ nanoparticle embedding for authentication of epoxy composites. *Advanced Materials* 30: 1801523.
38. Tan EKW, Shrestha PK, Pansare AV, et al. (2019) Density modulation of embedded nanoparticles via spatial, temporal, and chemical control elements. *Advanced Materials* 31: 1901802.
39. Montaseri H, Jamali F, Rogers JA, et al. (2004) The effect of temperature, pH, and different solubilizing agents on stability of taxol. *Iranian Journal of Pharmaceutical Sciences* 1: 43-51.
40. Williams WB, Cuvelier ME, Berset C (1995) Use of a free radical method to evaluate antioxidant activity. *LWT- Food Science and Technology* 28: 25-30.
41. Nicolaou KC, Riemer C, Kerr MA, et al. (1993) Design, synthesis and biological activity of protaxols. *Nature* 364: 464-466.
42. Pansare V, Kulal DK, Shedge AA, et al. (2016) hsDNA groove binding, photocatalytic activity, and in vitro breast and colon cancer cell reducing function of greener SeNPs. *Dalton Trans* 45: 12144-12155.
43. Pansare V, Chhatre SY, Khairkar SR, et al. (2020) "Shape-Coding": Morphology-based information system for polymers and composites. *ACS Appl Mater Interfaces*.
44. Khairkar SR, Pansare AV, Shedge AA, et al. (2020) Hydrophobic interpenetrating polyamide-PDMS membranes for desalination, pesticides removal and enhanced chlorine tolerance. *Chemosphere* 258: 127179.
45. Iqbal J, Abbasi BA, Mahmood T, et al. (2017) Plant-derived anticancer agents: A green anticancer approach. *Asian Pacific Journal of Tropical Biomedicine* 7: 1129-1150.
46. Khandel P, Yadav RK, Soni DK, et al. (2018) Biogenesis of metal nanoparticles and their pharmacological applications: Present status and application prospects. *Journal of Nanostructure in Chemistry* 8: 217-254.
47. Singh J, Dutta T, Kim KH, et al. (2018) Green synthesis of metals and their oxide nanoparticles: Applications for environmental remediation. *Journal of Nanobiotechnology* 16: 84.
48. Wu C, Gao Y, Liu Y, et al. (2018) Pure paclitaxel nanoparticles: Preparation, characterization, and antitumor effect for human liver cancer SMMC-7721 cells. *Int J Nanomedicine* 13: 6189-6198.
49. Chakravarthi SS, De S, Miller DW, et al. (2010) Comparison of anti-tumor efficacy of paclitaxel delivered in nano- and micro particles. *Int J Pharm* 383: 37-44.

50. Banstola, Pham TT, Jeong JH, et al. (2019) Polydopamine-tailored paclitaxel-loaded polymeric microspheres with adhered NIR-controllable gold nanoparticles for chemo phototherapy of pancreatic cancer. *Drug Deliv* 26: 629-640.
51. Xei J, Wang CH (2005) Self-assembled biodegradable nanoparticles developed by direct dialysis for the delivery of paclitaxel. *Pharm Res* 22: 2079-2090.
52. Calleja P, Esupelas S, Vauthier C, et al. (2015) Controlled release, intestinal transport, and oral bioavailability of paclitaxel can be considerably increased using suitably tailored pegylatedpoly (anhydride) nanoparticles. *J Pharm Sci* 104: 2877-2886.
53. Meenach SA, Anderson KW, Hilt JZ, et al. (2013) Characterization and aerosol dispersion performance of advanced spray-dried chemotherapeutic PEGylated phospholipid particles for dry powder inhalation delivery in lung cancer. *Eur J Pharm Sci* 49: 699-711.
54. Raja M, Subha J, Ali FB, et al. (2008) Synthesis of copper nanoparticles by electro reduction process. *Materials and Manufacturing Processes* 23: 782-785.
55. Pansare V, Kulal DK, Shedge AA, et al. (2016) Green synthesis of anti cancerous honeycomb PtNPs clusters: Their alteration effect on BSA and HsDNA using fluorescence probe. *Journal of Photochemistry and Photobiology B: Biology* 162: 473-485.
56. Pansare V, Shedge AA, Patil VR (2018) Discrete SeNPs-macromolecule binding manipulated by hydrophilic interaction. *Int J Biol Macromol* 107: 1982-1987.
57. Zhang G, Ma Y, Wang L, et al. (2012) Multispectroscopic studies on the interaction of maltol, a food additive, with bovine serum albumin. *Food Chemistry* 133: 264-270.
58. Pansare V, Shedge AA, Chhatre SY, et al. (2019) AgQDs employing black box synthetic strategy: Photocatalytic and biological behavior. *Journal of Luminescence* 212: 133-140.
59. Fraiji LK, Hayes DM, Werner TC (1992) Static and dynamic fluorescence quenching experiments for the physical chemistry laboratory. *Journal of Chemical Education* 69: 5.
60. Lakowicz JR (2006) Quenching of fluorescence. *Principles of Fluorescence Spectroscopy* 277-330.
61. Xu HN, Chen HJ, Zheng BY, et al. (2015) Preparation and sono dynamic activities of water-soluble tetra-a-(3-carboxyphenoxy) zinc(II) phthalocyanine and its bovine serum albumin conjugate. *Ultrasonic Sonochemistry* 22: 125-131.
62. Stan, Matei I, Mihailescu C, et al. (2009) Spectroscopic investigations of the binding interaction of a new indanedione derivative with human and bovine serum albumins. *Molecules* 14: 1614-1626.
63. Pyrzynska K, Pekal A (2013) Anal application of free radical diphenylpicrylhydrazyl (DPPH) to estimate the antioxidant capacity of food samples. *Methods* 5: 4288-4295.

DOI: 10.36959/525/450